**Atmospheric
Chemistry
and Physics
Discussions**

Estimates of mercury flux into the United States from non-local and global sources: results from a 3-D CTM simulation

B. A. Drewniak[1], V. R. Kotamarthi[1], D. Streets[2], M. Kim[3], and K. Crist[3]

[1]Environmental Science Division, Argonne National Laboratory, Argonne, IL, USA
[2]Decision and Information Sciences Division, Argonne National Laboratory, Argonne, IL, USA
[3]Department of Chemical Engineering, Ohio University, Athens, OH, USA

Correspondence to: V. R. Kotamarthi (vrkotamarthi@anl.gov)

ACPD

8, 19861–19890, 2008

**Mercury fluxes into
the US from non-local
and global sources**

B. A. Drewniak et al.

Title Page

Abstract	Introduction
Conclusions	References
Tables	Figures

|◄ | ►|

◄ | ►

Back | Close

Full Screen / Esc

Printer-friendly Version

Interactive Discussion

Abstract

The sensitivity of Hg concentration and deposition in the United States to emissions in China was investigated by using a global chemical transport model: Model for Ozone and Related Chemical Tracers (MOZART). Two forms of gaseous Hg were included in the model: elemental Hg (HG(0) and oxidized or reactive Hg (HGO). We simulated three different emission scenarios to evaluate the model's sensitivity. One scenario included no emissions from China, while the others were based on different estimates of Hg emissions in China. The results indicated, in general, that when Hg emissions were included, HG(0) concentrations increased both locally and globally. Increases in Hg concentrations in the United States were greatest during spring and summer, by as much as 7%. Ratios of calculated concentrations of Hg and CO near the source region in eastern Asia agreed well with ratios based on measurements. Increases similar to those observed for HG(0) were also calculated for deposition of HGO. Calculated increases in wet and dry deposition in the United States were 5–7% and 5–9%, respectively. The results indicate that long-range transcontinental transport of Hg has a non-negligible impact on Hg deposition levels in the United States.

1 Introduction

Mercury in the environment poses a risk to human health (NRC, 2000). Environmental Hg levels around the world have increased considerably in recent years, and even regions with no significant emissions, such as the Arctic, are affected by the transcontinental transport of Hg. Modeling studies and measurements have confirmed the ability of elemental Hg (HG(0) to be transported over long distances (Seigneur et al., 2001; Travnikov and Ryaboshapko, 2002; Banic et al., 2003; Dastoor and Larocque, 2004). This finding has generated concern in the United States that substantial quantities of long-range-transported atmospheric Hg might interfere with the ability of domestic sources to comply with future emission limitations (Steding and Flegal, 2002;

Seigneur et al., 2004). Mercury emissions from anthropogenic sources in rapidly growing economies in Asia and their impact on global Hg concentrations are of concern (Jaffe et al., 2005). Seigneur et al. (2004) estimated that anthropogenic emission of Hg in Asia contributed 21% of the total Hg deposition in the contiguous United States in 1998.

In this study, we coupled new emission inventories for China with a global chemical transport model (CTM) to perform a fresh assessment of the relative contributions of local and distant sources to Hg deposition in the United States. An existing global-scale three-dimensional (3-D) CTM, the Model for Ozone and Related Chemical Tracers (MOZART), was modified to include gas-phase Hg chemistry. Simulations were performed by using the National Center for Environmental Prediction (NCEP) assimilated dynamic fields for the year 2004. Several calculations were performed to test the sensitivity of US atmospheric Hg concentrations and deposition fluxes to a set of emission estimates from China, as follows:

- The first calculation was performed by using the global-scale emissions developed by Pacyna et al. (2006).

- A second estimate of emissions from China, developed by Streets et al. (2005), was substituted for the Pacyna et al. (2006) estimate in the second calculation.

- In a third calculation, we assign net zero emissions of Hg from China, while retaining the Pacyna et al. (2006) estimate for the rest of the world.

We present results from these simulations, particularly the expected contribution of sources in Asia to the US atmosphere. Our primary aim was to investigate the impact of this range of emissions from China on the United States, rather than focusing on uncertainties in the chemical mechanism leading to the formation of oxidized or reactive Hg (HGO) from HG(0).

Mercury fluxes into the US from non-local and global sources

B. A. Drewniak et al.

Full Screen / Esc

Printer-friendly Version

Interactive Discussion

2 Methods

2.1 Model framework

We used MOZART as described in Horowitz et al. (2003) and Wei et al. (2002), modified to include Hg chemistry. The grid resolution was based on meteorology data at 2.8 degrees latitude×2.8 degrees longitude, with 28 vertical levels extending from the surface to 2.7 mb. This model accounts for surface emissions (including N_2O, CH_4, CO, NO_x, NMHC, CH_2O, isoprene, acetone, etc.), chemical and photochemical reactions, advection, convection, and wet and dry deposition. The emission fluxes in MOZART for anthropogenic species were based on the Emission Database for Global Atmospheric Research (EDGAR) (Olivier et al., 1996). The version of MOZART used here provides spatial and temporal distributions for 52 chemical tracers, with a chemistry scheme similar to the one described by Brasseur et al. (1998), which incorporates 107 gas-phase, 5 heterogeneous, and 29 photochemical reactions. Empirical first-order heterogeneous reactions involving N_2O_5 and NO_3 on sulfate aerosols are implemented in the model (see Müller and Brasseur (1995) for details). Advection of the trace gases was simulated by using the flux-form semi-Lagrangian (FFSL) formulation of Lin and Rood (1996), which replaces the previous shape-preserving semi-Lagrangian scheme (Williamson and Rasch, 1989). The FFSL scheme is conservative and upstream biased. In addition, it contains monotonic constraints and conserves tracer correlations. Convective transport of trace gases was parameterized by using the schemes developed by Hack (1994) for shallow convection and by Zhang and McFarlane (1995) for deep convection, as in the National Center for Atmospheric Research Community Climate Model CCM3. Vertical diffusion with the boundary layer was represented by the parameterization of Holtslag and Bonville (1993). Dry deposition velocities for species including O_3, NO_x, HNO_3, PAN, organic nitrates, H_2O_2, organic peroxides, CH_2O, CH_3COCHO, CO, CH_3COCH_3, CH_4, and ^{210}Pb were computed from resistances specified as a sum of species-independent aerodynamic resistance and species-dependent surface resistance. MOZART also contains wet deposition of soluble

species (such as HNO_3, H_2O_2, CH_3OOH, C_3H_7OOH, C_3H_6OHOOH, CH_3COCH_2OOH, CH_3COOOH, C_2H_5OOH, HO_2NO_2, $CH_3COCHO_2CH_2OHNO$, CH_2O). For highly soluble gases (HNO_3 and H_2O_2), in-cloud scavenging and below-cloud scavenging by raindrops are included, as given by Brasseur et al. (1998). In-cloud scavenging is parameterized for all other species according to Giorgi and Chameides (1985). MOZART version 1 was described by Brasseur et al. (1998) and evaluated by Hauglustaine et al. (1998). We simulated one full year of Hg transport, driven with observed monthly meteorology data from NCEP for calendar year 2004. Multiyear simulations were created by running one year of data repeatedly until a steady state was achieved.

2.2 Mercury chemistry

The two Hg species currently included in the model are elemental mercury Hg(0) and HGO as the sum of all reactive mercury in the atmosphere. HGO represents the reactive mercury Hg(II) and reactive mercury that gets incorporated in particulate matter (HgP). Atmospheric chemistry for Hg is included in MOZART for Hg(0). The following reactions of Hg(0) with O_3, H_2O_2, and OH are included:

$$Hg(0) + O_3 \rightarrow HGO + O_2 \tag{R1}$$

$$Hg(0) + H_2O_2 \rightarrow Hg(OH)_2 \tag{R2}$$

$$Hg(0) + OH \rightarrow HGO \tag{R3}$$

The reaction rate for Reaction (R1) was set at 3×10^{-20} molec cm^{-3} s^{-1} on the basis of Hall (1995). The rate constant for Reaction (R2), leading to the production of Hg(OH)$_2$, was 8.5×10^{-19} molec cm^{-3} s^{-1} (Tokos et al., 1998), and the rate for Reaction (3) involving Hg(0) and OH was 8×10^{-14} molec cm^{-3} s^{-1} (Sommer et al., 2001; Pal and Ariya, 2004). All Hg in the model was considered to be emitted as Hg(0) at the surface. The dry deposition of Hg(0) was set to zero, as in other models, because dry deposition is relatively small and is assumed to be equivalent to soil re-emission (Bergan et

B. A. Drewniak et al.

al., 1999; Ryaboshapko et al., 2007). Wet deposition of Hg(0) was also set to zero, because Hg(0) is not very soluble in water.

Dry deposition of HGO was modeled with the parameters used for nitric acid (see Horowitz et al., 2003) because of the similar aqueous solubilities of these species. Wet deposition of HGO (like nitric acid) was represented as a first-order loss rate, on the basis of precipitation rates reported by Horowitz et al. (2003).

2.3 Emissions

The emission of Hg into the atmosphere is attributable to three different sources: natural emissions from land, natural emissions from oceans, and anthropogenic emissions. All surface emissions are assumed to be in all the form of Hg(0); these include 2000 $Mg\,y^{-1}$ from land and 2000 $Mg\,y^{-1}$ from oceans, evenly distributed over Earth's surface as described by Shia et al. (1999). Some more recent modeling studies have distributed natural Hg emissions according to locations of Hg mines and deposition patterns (Bergan et al., 1999; Seigneur et al., 2001; Seigneur et al., 2004; Selin et al., 2007). Because we are only interested in changes in concentration and deposition due to anthropogenic Hg sources, and natural emissions primarily increase background concentrations, we did not include the spatial distribution of natural emissions in our model.

Anthropogenic Hg emissions were spatially distributed according to three cases:

1. *Pacyna*: Anthropogenic emissions derived from Pacyna et al. (2006).

2. *No China*: Same as *Pacyna* but with anthropogenic emissions from China set to zero.

3. *Streets*: Same as *Pacyna* but with emissions from China based on Streets et al. (2005).

The *No China* and the *Streets* cases had identical emissions except for China. The *Pacyna* case had higher emissions than the *Streets* case for China. Figure 1 shows the

difference between Streets et al. (2005) emissions and Pacyna et al. (2006) emissions for China. For all Hg sources in China, Streets et al. (2005) estimated 16.5% lower emissions. Total annual anthropogenic emissions for the three cases were as follows: 2207 Mg y^{-1} for the *Pacyna* case, 1578 Mg y^{-1} for the *No China* case, and 1935 Mg y^1

5 for the *Streets* case. Initial conditions of background Hg concentrations were assumed to be 1.5 ng m^{-3} (Ebinghaus et al., 2001; Weiss-Penzias et al., 2003; Swartzendruber et al., 2006) in the form of Hg(0), distributed evenly over Earth's surface and through all layers of the atmosphere (Slemr et al., 1985). Background concentrations of HGO were set to zero initially, because HGO has a short lifetime, and the model reaches

10 steady state quickly.

3 Results

3.1 Elemental mercury

The global background concentrations of Hg(0) calculated by our model are shown in Fig. 2 for the *Pacyna* emissions case, as described in Sect. 2.3. Model results are

15 shown for surface grid levels as averages for the four Northern Hemisphere seasons of winter, spring, summer, and fall. For all seasons, concentrations of Hg(0) were highest for China, with values of 4 ng m^{-3} and more. Much of the Northern Hemisphere experiences concentrations on the order of 2–3 ng m^{-3} during winter and fall. Seasonal trends show the greatest Hg(0) concentrations during winter and the smallest concen-

20 trations in summer, consistent with previous observations (Iverfeldt, 1991; Ames et al., 1998; Ebinghaus et al., 2001; Kellerhals et al., 2003; Poissant et al., 2005; Stamenkovic et al., 2007). Figure 3 compares model-calculated and measured Hg(0) in July–December 2004 at a site in the central Ohio River valley in Athens, Ohio (Yatavelli et al., 2006). The site is at approximately 900 ft above sea level and is on a small hill, at

25 a height of 250 ft above the surrounding terrain. The model results shown are for a grid location at 950 mb, which is approximately 250 ft above the model surface. In general,

the model-calculated concentrations are higher than measured values but within the range of the measurement variability.

Figure 4 shows the percent difference in surface concentrations of Hg(0) between the *Streets* and *No China* simulations. Although the greatest difference is centered near and over China, evidence of transport in the Northern Hemisphere is suggested by the ubiquitous increases in Hg(0), with more widespread transport during spring and summer. The spring transport causes Hg(0) concentrations to increase by up to 7% in parts of the western United States and 3–5% in the eastern United States. Background concentrations in the Southern Hemisphere are also affected, although the effect is small, with an increase of less than 1%. The average increase in Hg concentrations globally is 3–4%.

Comparison of the *Pacyna* and *Streets* simulations (Fig. 5) also indicates an increase in percent difference of Hg concentrations, although the increase is smaller than for the *Streets* and *No China* comparison (Fig. 4). In spring and summer, patterns for the *Pacyna-Streets* comparison (Fig. 5) are similar to those for the *Streets-No China* comparison (Fig. 4), with an increase in concentrations that extends throughout the Northern Hemisphere and smaller increases in the Southern Hemisphere. The variability of Hg concentration in South Africa, Australia, and Europe (Fig. 5) is the result of differences in gridding the emission distribution input to MOZART. Although most of these effects are localized and most of the variations offset each other, they do have an impact on the regional Hg budget. Nevertheless, the effects do not make a large contribution to the global Hg budget (except for South Africa and Australia, where a few differences do not offset each other and cause an increase in Hg concentrations in excess of 1% in the Southern Hemisphere). For example, in the spring certain regions in the eastern United States have Hg concentrations that are 10% higher in the *Pacyna* simulation than in *Streets* simulation. These pockets of high Hg concentration are small and occur near regions where anthropogenic emissions do not agree between the two simulations.

Previous studies have addressed the relationship between Hg and CO, because both

Full Screen / Esc

Printer-friendly Version

Interactive Discussion

are emitted through industrial processes, have similar lifetimes, and can be transported long distances in the atmosphere (Jaffe et al., 2005; Friedli et al., 2004; Weiss-Penzias et al., 2007). Figure 6 shows a time series for 22 March–10 June 2004, of calculated CO and Hg(0) concentrations near Okinawa. We chose this time period because it falls within the observations of Jaffe et al. (2005), and spring corresponds to peak continental outflow in the western Pacific. To improve representation of episodic transport events, we removed the contribution of background emissions by subtracting *No China* Hg(0) from *Streets* Hg(0). The largest transport events occurred in April and May, and several corresponded to events observed by Jaffe et al. (2005). For example, Jaffe et al. (2005) observed a large transport event on 20 April 2004 (day 111), while MOZART calculated a transport event on 21 April 2004 (day 112). Figure 7 shows the same time series for a location near Seattle, Washington. In this case, subtraction of the *No China* Hg(0) from *Streets* Hg(0) revealed no episodic transport events. Mercury from China in the atmosphere seems to be fairly well mixed into the background when it has migrated this distance from the source.

Figures 8 and 9 are plots of calculated concentration ratios (Hg(0):CO) from the *No China* and *Streets* simulations, respectively. The slopes for the regression lines of these two graphs are $0.0043\,\mathrm{ng\,m^{-3}\,ppbv^{-1}}$ for the *No China* simulation (Fig. 8) and $0.0056\,\mathrm{ng\,m^{-3}\,ppbv^{-1}}$ for the *Streets* simulation (Fig. 9). These values correspond well with results for observations of Jaffe et al. (2005) (slope=$0.0053\,\mathrm{ng\,m^{-3}\,ppbv^{-1}}$) and the ACE-Asia field campaign (Friedli et al., 2004) (slope=$0.0056\,\mathrm{ng\,m^{-3}\,ppbv^{-1}}$). The calculated values for Hg(0) and CO in Figs. 8 and 9 are well correlated, with R^2 values of 0.80 for the *No China* simulation and 0.89 for the *Streets* simulation. The difference in the values for correlation of determination is caused by the variability of Hg(0), rather than CO, between simulations. Because Hg(0) was the only pollutant from China that was altered, the *No China* simulation was expected to have a lower correlation. The slope calculated in the *Streets* simulation is indicative of transport from China; it corresponds well to the value calculated by Jaffe et al. (2005) from observations.

3.2 Reactive mercury

To evaluate the model-calculated HGO, we analyzed wet and dry deposition, as discussed below. Results from all the three scenarios discussed in Sect 2.3 are used for the analysis.

3.2.1 Wet deposition

Wet deposition is highly seasonal, being highest in spring and lowest in fall. Observations suggest that wet deposition is usually low during winter in the United States. The calculated wet deposition is high during winter in MOZART simulations because of large concentrations of HGO at that time. Seasonal wet deposition differences between the *Streets* and *No China* simulations are shown in Fig. 10. The differences are concentrated over China, with evidence of global transport, particularly during the summer. During winter and fall, decreased transport causes a large flux of HGO deposition over China. During spring and summer, strong winds allow Hg to cross the Pacific Ocean and become well mixed with the air in the Northern Hemisphere. Thus, during spring and summer an increase in wet deposition occurs throughout the entire Northern Hemisphere. This increase in wet deposition amounts to 7–8% in the eastern and western United States, with larger changes in portions of the western United States. In the Southern Hemisphere, wet deposition of HGO increases globally by an average of 2%. The largest increase in deposition away from the source occurs in spring, when transport is strongest and outflow from western Pacific is dominant. However, the generally greater wet deposition during this season makes the percent increases in wet deposition small. The opposite is true for the fall – though the amount of wet-deposited HGO changes little between simulations, the percent increase is large, because little wet deposition occurs in the fall.

Differences in wet deposition between the *Pacyna* and *Streets* simulations for the spring and summer months are shown in Fig. 11. The impact of a slight increase in emission amounts from China is small. As with the *Streets-No China* comparison

(Fig. 10), the biggest increase in emissions in the *Pacyna-Streets* comparison (Fig. 11) occurs during the spring; however, the largest percent change occurs during the summer because of the smaller wet deposition in summer. Again, both seasons show transport, with wet deposition increases of 4% over the United States and Canada during the summer. During the spring, the percent difference is 2% over the entire United States. The Southern Hemisphere has a difference of less than 1–2%.

3.2.2 Dry deposition

Dry deposition patterns are very similar to the wet deposition patterns. In general, dry deposition peaks in spring in the Northern Hemisphere and in fall in the Southern Hemisphere.

For dry deposition, the percent difference between the *Streets* and *No China* simulations is shown in Fig. 12. The largest percent change in dry deposition occurred over China during the winter and fall, when the year's smallest outflow into the western Pacific allowed Hg to be deposited near its source. However, the change in dry deposition during the spring and summer showed a more global increase. Ready transport across the Northern Hemisphere during these seasons allowed larger differences in deposition patterns between simulations, especially during the spring when transport is the highest. During the spring, differences in dry deposition increased by 7–8% in the western United States and by 6–7% in the eastern United States. During the summer, differences in dry deposition increased by 7–9% in the western United States, by >9% in the far northwestern United States, and by 5–6% in the eastern United States. The change in dry deposition was generally less than 1% in the Southern Hemisphere.

Although both summer and fall seasons showed large percent increases in dry deposition, absolute differences between *Streets* and *No China* were smallest during these months because of the low rates of dry deposition during this period (Sect. 3.3.1). Figure 13 shows the percent difference between the *Pacyna* and *Streets* simulations for spring and summer. As with wet deposition, the increase in differences for the China emissions was smaller during these months. Large increases in deposition differences

occurred during spring, although the percent change was small because dry deposition was high. During the summer, a more pronounced increase occurred, particularly over China, but the pattern also extended through the Pacific Ocean and into the northwestern United States. Spring increases in differences in dry deposition were 4% over the United States. During the summer, the percent change in dry deposition was much greater in the northern United States (6%) than in the southern United States (4%). Increases in the Southern Hemisphere amounted to 1–2% for all seasons.

4 Conclusions

We used the chemical transport model MOZART with two additional constituents – Hg(0) and HGO – as transported species. The model was used to evaluate the sensitivity of calculated Hg(0) and HGO over the United States to anthropogenic emissions in China. The model-calculated Hg concentrations, in general, fell into the range of current observations. Concentrations of Hg(0) are seasonal, with high values during the winter and low values during the spring. Ratios of Hg(0):CO also show that the model does capture the relationship between Hg and the CO tracer, demonstrating the model's ability to simulate the correct Hg(0) pattern. Deposition of Hg is also seasonal, with peaks in the springtime and minimum values during the fall. With decreased or increased emissions from China, changes in concentration and deposition are experienced globally. Large changes occur locally during winter and fall, and changes in transport occur during spring and summer. Including emissions from China in the simulations increased calculated Hg concentrations in the United States by up to 7%.

Uncertainties in Hg emissions and distribution (both anthropogenic and natural) are still significant, creating difficulties in estimating the circulation of Hg. Wu et al. (2006) found that Hg emissions from China are increasing at a rate of about 3% per year. In addition, the much higher Hg emission rates from China estimated by Jaffe et al. (2005) and Weiss-Penzias et al. (2007) could be explained by missing or underestimated sources, such as underreported point sources, natural sources, re-emission, and er-

Mercury fluxes into the US from non-local and global sources

B. A. Drewniak et al.

Full Screen / Esc

Printer-friendly Version

Interactive Discussion

rors in emission fractions. Some of the missing or underestimated emissions have been accounted for as originating in natural sources, through an evaluation of emissions by vegetation, soil, and water by Shetty et al. (personal communication, 2008). Including these new estimates would lead to an increase in transport to the western United States, as well as an increase in the global background of Hg. Other studies have demonstrated the effect of aqueous chemistry on Hg concentrations and deposition (Shia et al., 1999; Seigneur et al., 2006). Including aqueous chemistry can increase Hg(0) concentrations by a factor of 2–4 (Seigneur et al., 2006) and decrease wet and dry deposition of HGO by 18% and 9%, respectively (Shia et al., 1999). To improve understanding of the Hg cycle, we will address this chemistry and will also incorporate a better estimate of Hg emissions in future work.

References

Ames, M., Gullu, G., and Olmex, I.: Atmospheric mercury in the vapor phase, and in fine and coarse particulate matter at Perch River, New York, Atmos. Environ., 32, 865–872, 1998.

Banic, C. M., Beauchamp, S. T., Tordon, R. J., Schroeder, W. H., Steffen, A., Anlauf, K. A., and Wong, H. K. T.: Vertical distribution of gaseous Hg(0) in Canada, J. Geophys. Res., 108(D9), 4264, doi:10.1029/2002JD002116, 2003.

Bergan, T., Gallardo, L., and Rodhe, H.: Mercury in the global troposphere: A three-dimensional model study, Atmos. Environ., 33, 1575–1585, 1999.

Brasseur, G. P, Hauglustaine, D. A., Walters, S., Rasch, P. J., Muller, J.-F., Ganier,C., and Tie, X. X., MOZART: A global chemical transport model for ozone and related chemical tracers – Part 1, Model description, J. Geophys. Res., 103, 28 265–28 289,1998.

Dastoor, A. P. and Larocque, Y.: Global circulation of atmospheric mercury: A modeling study, Atmos. Environ., 38, 147–161, 2004.

Ebinghaus, R., Kock, H. H., and Schmolke, S. R.: Measurements of atmospheric mercury with

Mercury fluxes into the US from non-local and global sources

B. A. Drewniak et al.

Title Page

Abstract | Introduction

Conclusions | References

Tables | Figures

◄ | ►

◄ | ►

Back | Close

Full Screen / Esc

Printer-friendly Version

Interactive Discussion

high time resolution: Recent application in environmental research and monitoring, Fresen, J. Anal. Chem., 371, 806–815, 2001.

Friedli, H. R., Radke, L. F., Prescott, R., Li, P., Woo, J. H., and Carmichael, G. R.: Mercury in the atmosphere around Japan, Korea, and China as observed during the 2001 ACE-Asia field campaign: Measurements, distributions, sources, and implications, J. Geophys. Res., 109, D19S25, doi:10.1029/2003JD004244, 2004.

Giorgi F. and Chameides, W. L.: The rainout parameterization in a photochemical model, J. Geophys. Res., 90, 7872–7880, 1985.

Hack J. J.: Parameterization of moist convection in the National Center of Atmospheric Research Community Model (CCM2), J. Geophys. Res., 99, 5551–5568, 1994.

Hall, B.: The gas-phase oxidation of elemental mercury by ozone, Water Air Soil Poll., 80, 235–250, 1995.

Hall, B. and Bloom, N.: Report to EPRI, Electric Power Research Institute, Palo Alto, Calif., 1993.

Hauglustaine, D. A., Brasseur, G. P., Walters, S., Rasch, P. J., Muller, J.-F., Emmons, L. K., and Carroll, M. A., MOZART: A global chemical transport model for ozone and related chemical tracers – Part 2: Models results and evaluations, J. Geophys. Res.,103, 28 291–28 335, 1988.

Holtslag, A. and B. Boville: Local versus nonlocal boundary-layer diffusion in a global climate model, J. Clim., 6, 1825–1842, 1993.

Horowitz, L. W., Walters, S., Mauzerall, D. L., Emmons, L. K., Rasch, P. J., Granier, C., Tie, X., Lamarque, J. F., Schultz, M. G., Tyndall, G. S., Orlando, J. J., and Brasseur, G. P.: A global simulation of tropospheric ozone and related tracers: Description and evaluation of MOZART, version 2, J. Geophys. Res., 108, 4784, doi:10.1029/2002JD002853, 2003.

Iverfeldt, Å.: Occurrence and turnover of atmospheric mercury over the Nordic countries, Water Air Soil Poll., 56, 251–265, 1991.

Jaffe, D., Prestbo, E., Swartzendruber, P., Weiss-Penzias, P., Kato, S., Takami, A., Hatakeyama, S., and Kajii, Y.: Export of atmospheric mercury from Asia, Atmos. Environ., 39, 3029–3038, 2005.

Kellerhals, M., Beauchamp, S., Belzer, W, Blanchard, P., Froude, F., Harvey, B., McDonald, K., Pilote, M., Poissant, L., Puckett, K., Schroeder, B., Steffen, A., and Tordon, R.: Temporal and spatial variability of total gaseous mercury in Canada: Results from the Canadian Atmospheric Measurement Network (CAMNet), Atmos. Environ., 37, 1003–1011, 2003.

Lin, S.-J. and Rood, R. B.: Multidimensional flux-form semi-Lagrangian transport schemes, Mon. Wea. Rev., 124, 2046–2070, 1996.

Müller, J.-F. and Brassuer, G.: IMAGES: A three-dimensional chemical transport model for the global atmosphere, J. Geophys. Res., 100, 16 445–16 490, 1995.

National Research Council, Toxicological Effects of Methylmercury, Committee on the toxicological effects of Methylmercury, National Academy Press, Washington, DC, 2000.

Olivier, J. G. J., Bouwman, A. F.,van der Maas, C. W. M. , Berdowski, J. J. M., Veldt, C., Bloos, J. P. J., Visschedijk, A. J. H., Zandveld, P. Y. J., and Haverlag, J. L.: Description of EDGAR Version 2.0: A set of Global Emission Inventories of Greenhouse Gases and Ozone-Depleting Substances for All Anthropogenic and Most Natural Sources on a Per Country Basis and on a 1×1 degree grid, RIVM report 771060 002/TNO-MEP report R96/119, National Institute of Public Health and the Environment, Bilthoven, The Netherlands, 1996.

Pacyna, E. G., Pacyna, J. M., Steenhuisen, F., and Wilson, S.: Global anthropogenic mercury emission inventory for 2000, Atmos. Environ., 40, 4048–4063, 2006.

Pal., B. and Ariya, P. A.: Gas-phase HO-initiated reactions of elemental mercury: Kinetics, product studies and atmospheric implications, Environ. Sci. Technol., 38, 5555–5566, 2004.

Poissant, L., Pilote, M., Beauvais, C., Constant, P., and Zhang, H. H.: A year of continuous measurements of three atmospheric mercury species (GEM, RGM, and Hg_p) in southern Quebec, Canada, Atmos. Environ., 39, 1275–1287, 2005.

Ryaboshapko, A., Bullock Jr., O. R., Christensen, J., Cohen, M., Dastoor, A., Ilyin, I., Peterson, G., Syrakov, D., Travnikov, O., Artx, R. S., Davignon, D., Draxler, R. R., Munthe, J., and Pacyna, J.: Intercomparison study of atmospheric mercury models: 2. Modeling results vs. long-term observations and comparison of country deposition budgets, Sci. Total Environ., 377, 319–333, 2007.

Seigneur, C., Karamchandani, P., Lohman, K., Vijayaraghavan, K., and Shia, R.-L.: Multiscale modeling of the atmospheric fate and transport of mercury, J. Geophys. Res., 106(D21), 27 795–27 809, 2001.

Seigneur, C., Vijayaraghavan, K., Lohman, K., Karamchandani, P., and Scott, C.: Global source attribution for mercury deposition in the United States, Environ. Sci. Technol., 38(2), 555–569, 2004.

Seigneur, C., Vijayaraghavan, K., and Lohman, K.:, Atmospheric mercury chemistry: Sensitivity of global model simulations to chemical reactions, J. Geophys. Res., 111, D22306, doi:10.1029/2005JD006780, 2006.

Mercury fluxes into the US from non-local and global sources

B. A. Drewniak et al.

Title Page

Abstract | Introduction

Conclusions | References

Tables | Figures

◄◄ | ►►

◄ | ►

Back | Close

Full Screen / Esc

Printer-friendly Version

Interactive Discussion

Selin, N. E., Jacob, D. J., Park, R. J., Yantosca, R. M., Strode, S., Jaegle L., and Jaffe, D.: Chemical cycling and deposition of atmospheric mercury: Global constraints from observations, J. Geophys. Res., 112, D02308, doi:10.1029/2006JD007450, 2007.

Shia, R.-L., Seigneur, C., Pai, P., Ko, M., and Sze, N. D.: Global simulation of atmospheric mercury concentrations and deposition fluxes, J. Geophys. Res., 104, 23 747–23 760, 1999.

Slemr, F., Schuster, G., and Seiler, W.: Distribution, speciation, and budget of atmospheric mercury, J. Atmos. Chem., 3, 407–434, 1985.

Sommer, J., Gårdfeldt, K., Strömberg, D., and Feng, X.: A kinetic study of the gas-phase reaction between the hydroxyl radical and atomic mercury, Atmos. Environ., 35, 3049–3054, 2001.

Stamenkovic, J., Lyman, S., and Gustin, M. S.: Seasonal and diel variation of atmospheric mercury concentrations in the Reno (Nevada, USA) airshed, Atmos. Environ., 41, 6662–6672, 2007.

Steding, D. J. and Flegal, A. R.: Mercury concentrations in coastal California precipitation: evidence of local and trans-Pacific fluxes of mercury to North America, J. Geophys. Res., 107(D24), 4764, doi:10.1029/2002JD002081, 2002.

Streets, D. G., Jiming, H., Wu, Y., Jiang, J., Chan, M., Tian, H., and Feng, X.: Anthropogenic mercury emissions in China, Atmos. Environ., 39, 7789–7806, 2005.

Swartzendruber, P. C., Jaffe, D. A., Prestbo, E. M., Weiss-Penzias, P., Stelin, N. E., Park, R., Jacob, D. J., Strode, S., and Jaegle, L.: Observations of reactive gaseous mercury in the free troposphere at the Mount Bachelor Observatory, J. Geophys. Res., 111, D24301, doi:10.1029/2006JD007415, 2006.

Tokos, J. S. S., Hall, B., Calhoun, J. A., and Prestbo, E. M.: Homogeneous gas-phase reaction of HGO with H_2O_2, O_3, CH_3I, and $(CH_3)_2S$: Implication for atmospheric Hg cycling, Atmos. Environ., 32, 823–827, 1998.

Travnikov, O. and Ryaboshapko, A.: Modelling of mercury hemispheric transport and depositions. MSC-E Technical Report 6/2002, Meteorological Synthesizing Centre-East, Moscow, Russia, 67 pp., 2002.

Williamson D. L. and Rasch, P. J.: Two dimensional, semi-Lagrangian transport with shape preserving interpolation, Mon. Weather Rev., 117, 102–129, 1989.

Wei, C. F., Kotamarthi, V. R., Ogunsola, O. J., Horowitz, L. W., Walters, S., Wuebbles, D. J.,Avery, M. A., Blake,D. R., Browell, E. V., and Sachse, G. W.: Seasonal variability of ozone mixing ratios and budgets in the tropical southern Pacific: A GCTM perspective, J. Geophys.

Mercury fluxes into the US from non-local and global sources

B. A. Drewniak et al.

Research, 108(D2), 8235, doi:10.1029/2001JD000772, 2003.

Weiss-Penzias, P., Jaffe, D. A., McClintick, A., Prestbo, E. M., and Landis, M. S.: Gaseous elemental mercury in the marine boundary layer: Evidence for rapid removal in anthropogenic pollution, Environ. Sci. Technol., 37, 3755–3763, 2003.

5 Weiss-Penzias, P., Jaffe, D., Swartzendruber, P., Hefner, W., Chanol, D., and Prestbo, E.: Quantifying Asian and biomass burning sources of mercury using the Hg/CO ratio in pollution plumes observed at the Mount Bachelor observatory, Atmos. Environ., 41(21), 4366–4379, 2007.

Wu, Y., Wang, S., Streets, D. G., Hao, J., Chan, M., and Jiang, J.: Trends in anthropogenic
10 mercury emissions in China from 1995 to 2003, Environ. Sci. Technol., 40, 5312–5318, 2006.

Yatavelli, R. L. N., Fahrni, J. K., Kim, M., Crist, K. C., and Vickers, C. D.: Mercury, PM2.5 and gaseous co-pollutants in the Ohio River Valley region: Preliminary results from the Athens supersite, Atmos. Environ., 40, 6650–6665, 2006.

15 Zhang, G. J. and McFarlane, N. A.: Sensitivity of climate simulations to the parameterization of cumulus convection in the Canadian Climate Center general circulation model, Atmos. Ocean, 33, 407–446, 1995.

Mercury fluxes into the US from non-local and global sources

B. A. Drewniak et al.

Title Page

Abstract | Introduction

Conclusions | References

Tables | Figures

◄ | ►

◄ | ►

Back | Close

Full Screen / Esc

Printer-friendly Version

Interactive Discussion

Updated total mercury emission of China, 2000
(Argonne - Pacyna)
(Citation: Argonne)

Ohio University Air Quality Center

(kg per 0.5 ° X 0.5 ° grid)

<-5000.00 (Min: -6558)	-500.00 - -100.00	-0.10 - 0.00	50.00 - 100.00	1000.00 - 5000.00
-5000.00- -1000.00	-100.00 - -50.00	0.00 - 0.10	100.00 - 500.00	5000.00 - 10000.00
-1000.00 - -500.00	-50.00 - -0.10	0.10 - 50.00	500.00 - 1000.00	>10000 (Max:35043)
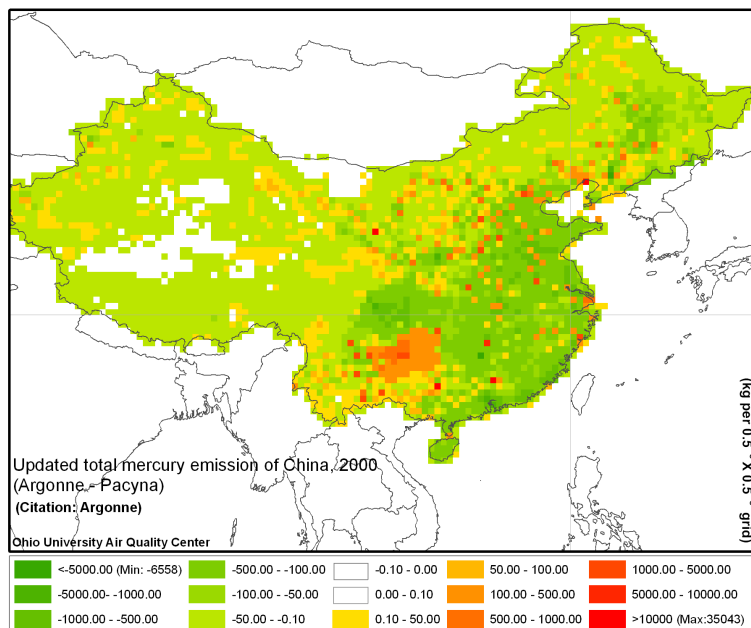
Fig. 1. Differences between the lower Streets et al. (2005) and higher Pacyna et al. (2006) estimates of anthropogenic emissions for China.
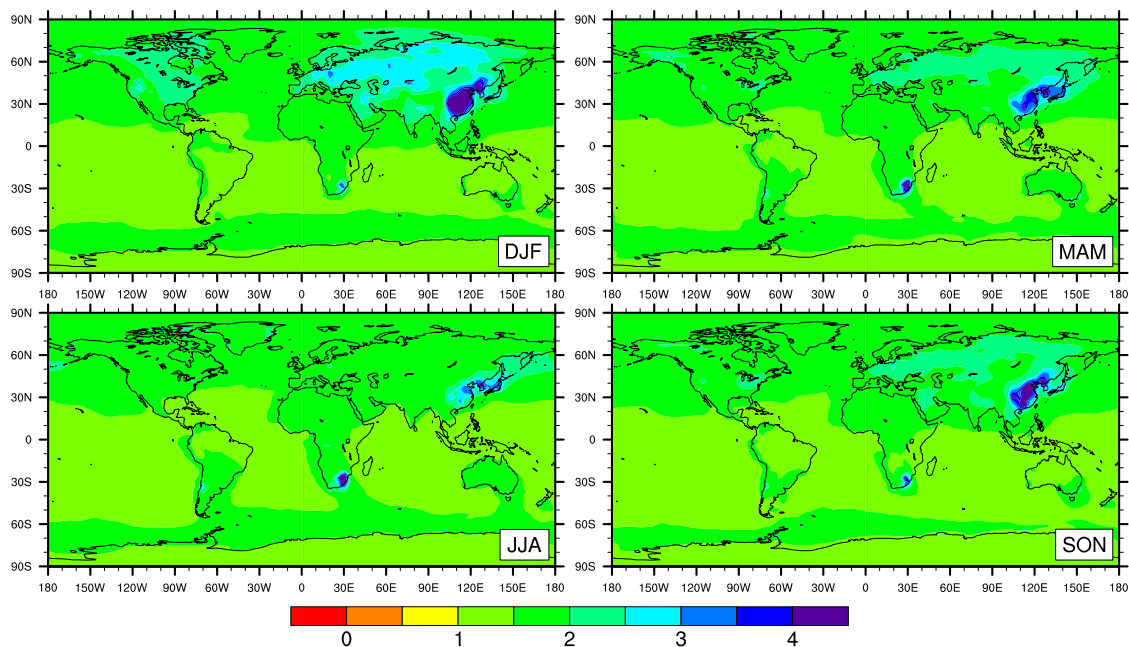
Fig. 2. Model-calculated background Hg(0) concentrations (ng m^{-3}) at the model surface for the Northern Hemisphere in winter (upper left), spring (upper right), summer (lower left), and fall (lower right), in the *Pacyna* emissions case.
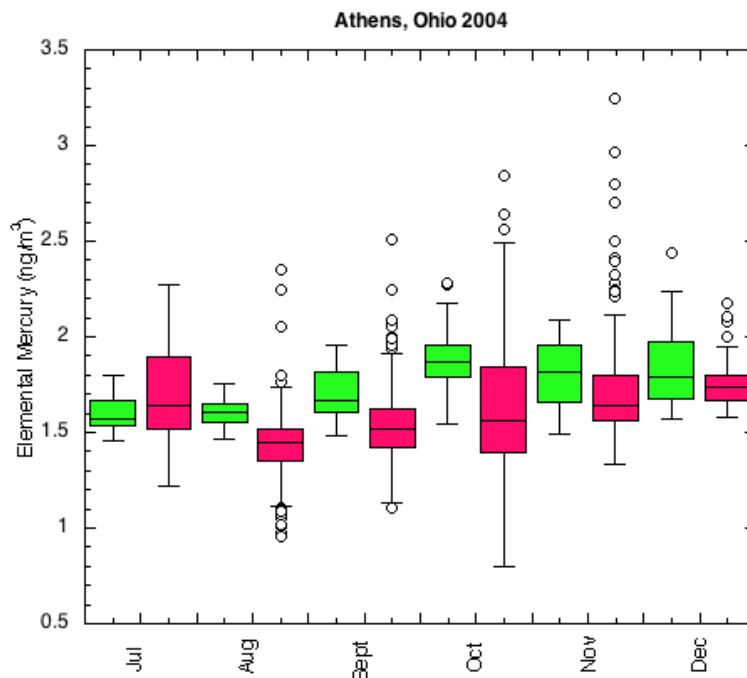
Fig. 3. Observed and modeled concentrations of Hg(0) for a model grid located over Athens, Ohio, USA. The site is located at a height of 900 ft above sea level and approximately about 250 ft above the surrounding terrain. The model results (green) are for an altitude of 950 mb above the model surface pressure of 995 mb. The observations shown are for the year 2004 (the year simulated with the model); the site became operational in July 2004 (Yatavelli et al., 2006).
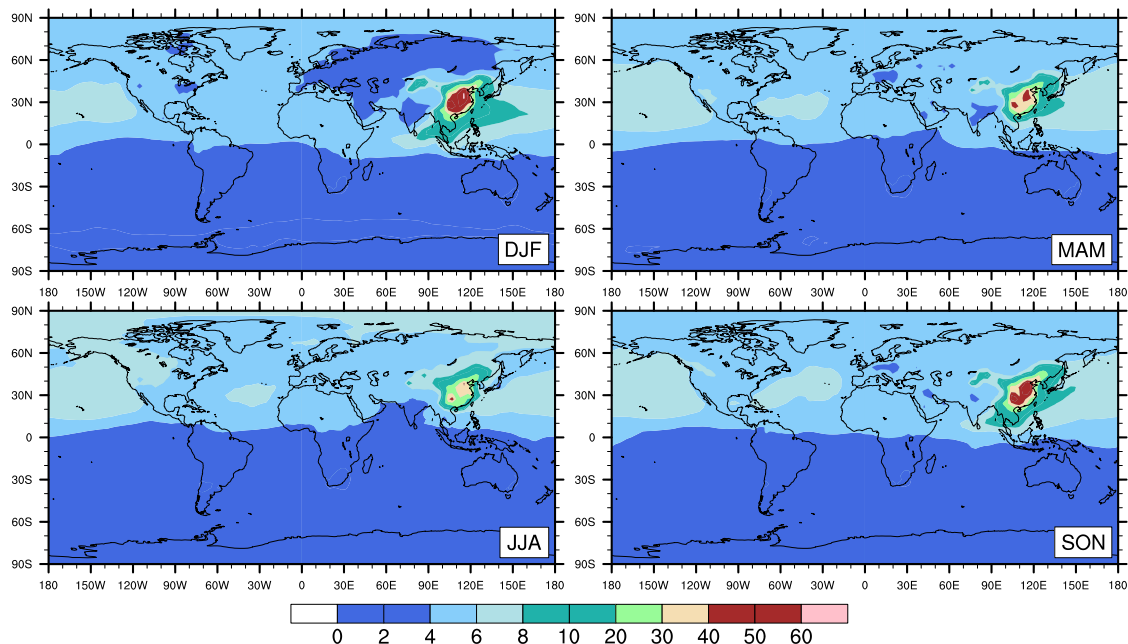
Fig. 4. Percent difference in Hg(0) concentrations between a simulation using the Hg(0) emissions estimate of Streets et al. (2006) and a simulation with no emissions from China. Results for the Northern Hemisphere are shown at the model surface in winter (upper left), spring (upper right), summer (lower left), and fall (lower right).

Full Screen / Esc
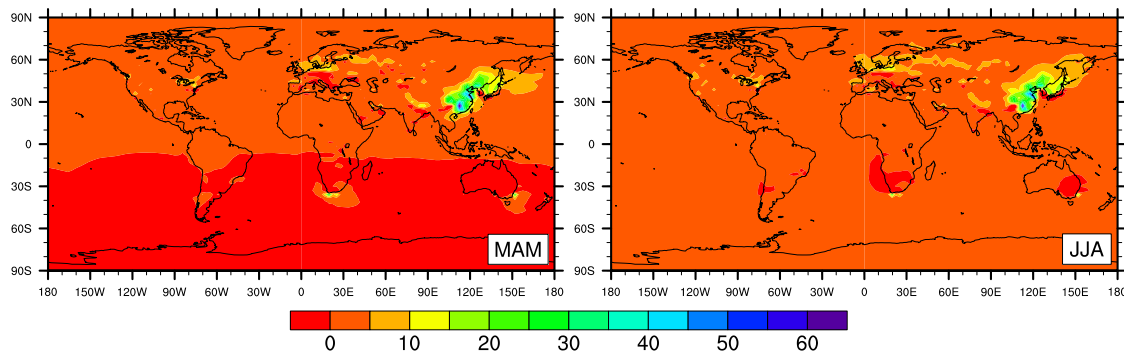
Fig. 5. Percent difference in Hg(0) concentrations in spring (left) and summer (right), as simulated with the *Pacyna* and *Streets* estimates of Hg emissions.
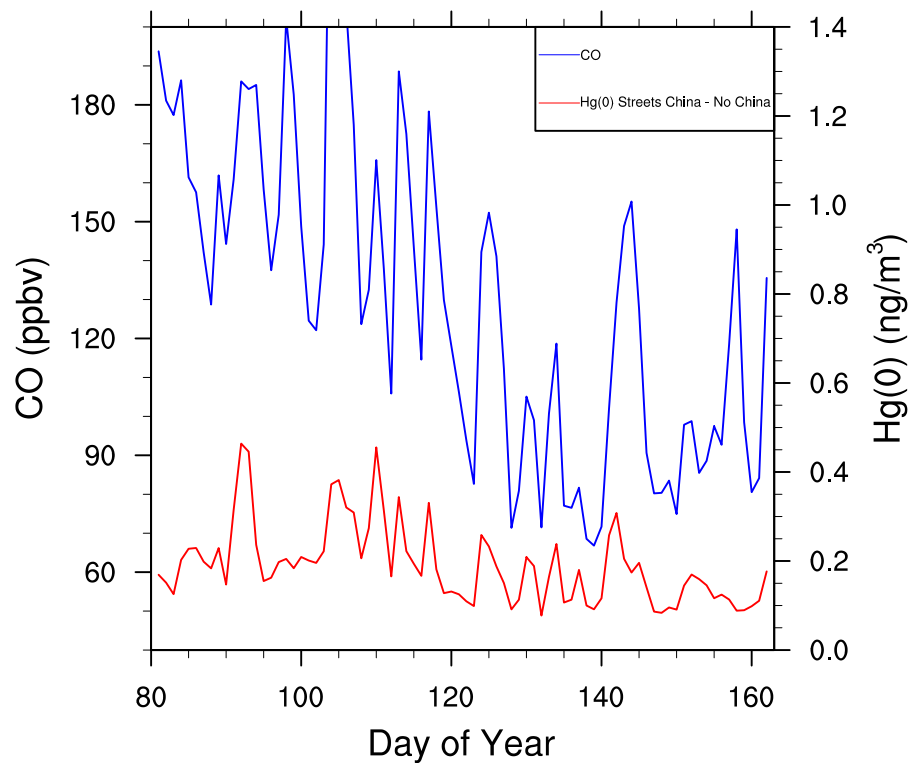
Fig. 6. Calculated concentrations of CO (ppbv) and Hg(0) (ng m^{-3}) near Okinawa for the period 22 March–10 June 2004.
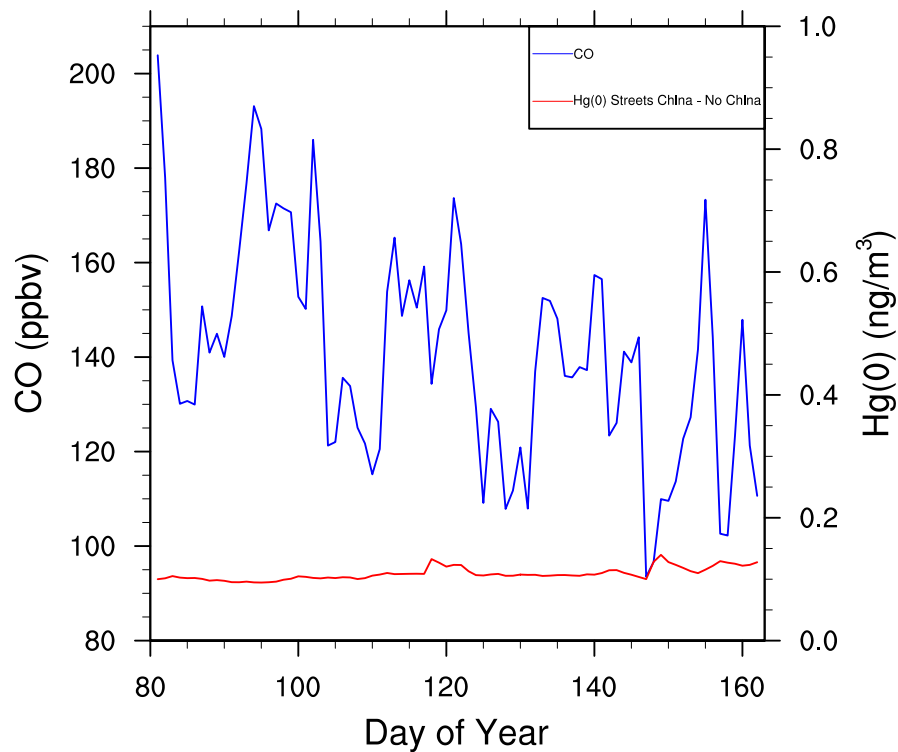
Fig. 7. Calculated concentrations of CO (ppbv) and Hg(0) ($ng\,m^{-3}$) near Seattle, Washington, for the period 22 March–10 June 2004.
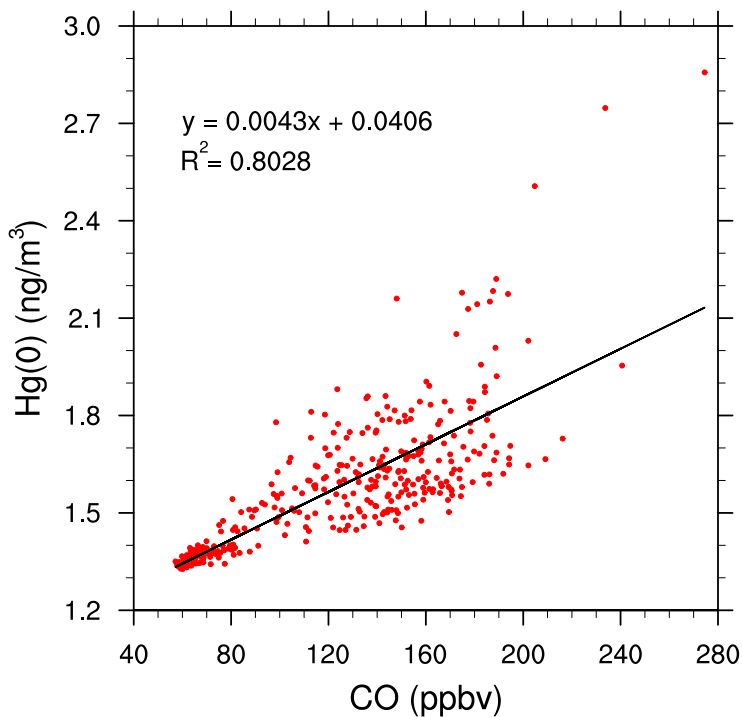
Fig. 8. Scatter plot of calculated Hg(0) ($\mathrm{ng\,m^{-3}}$) vs. CO concentrations (ppbv) near Okinawa for the period 22 March–10 June 2004, and the *No China* simulation.
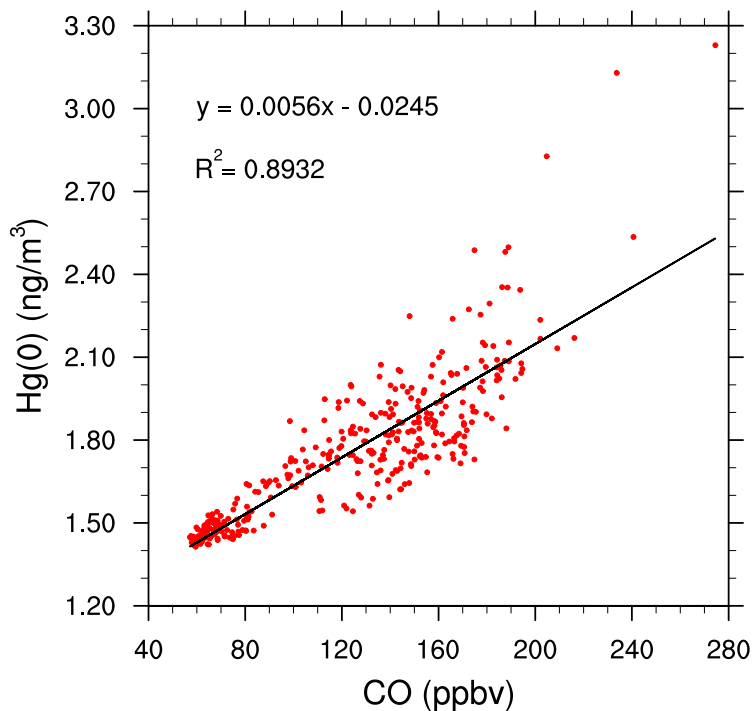
Fig. 9. Scatter plot of calculated Hg(0) $(ng\,m^{-3})$ vs. CO (ppbv) concentrations near Okinawa for the period 22 March–10 June 2004, and the *Streets* simulation.

Full Screen / Esc

Printer-friendly Version

Interactive Discussion
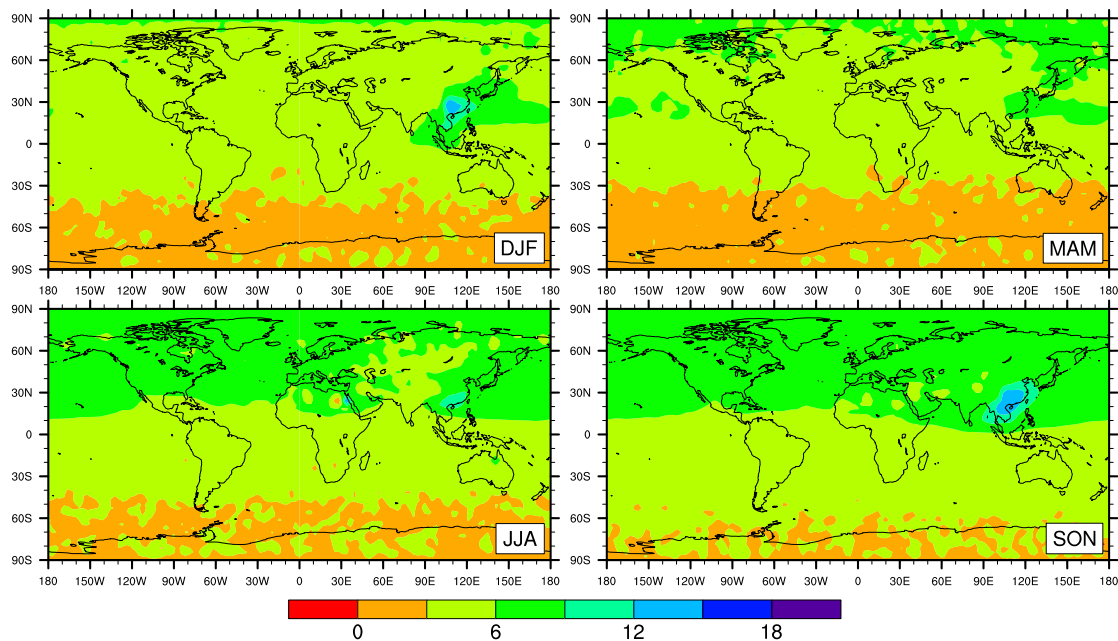
Fig. 10. Percent differences in HGO wet deposition in winter (upper left), spring (upper right), summer (lower left), and fall (lower right) for the *Streets* and *No China* simulations.
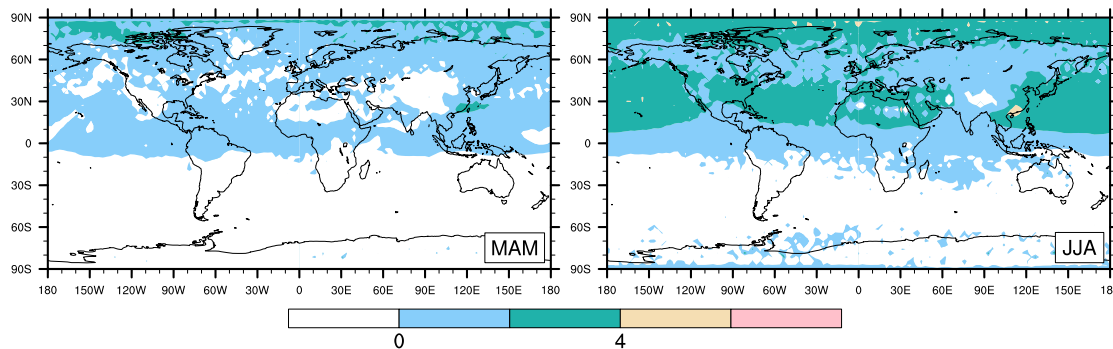
Fig. 11. Percent differences in HGO wet deposition in spring (left) and summer (right) for the *Pacyna* and *Streets* simulations.
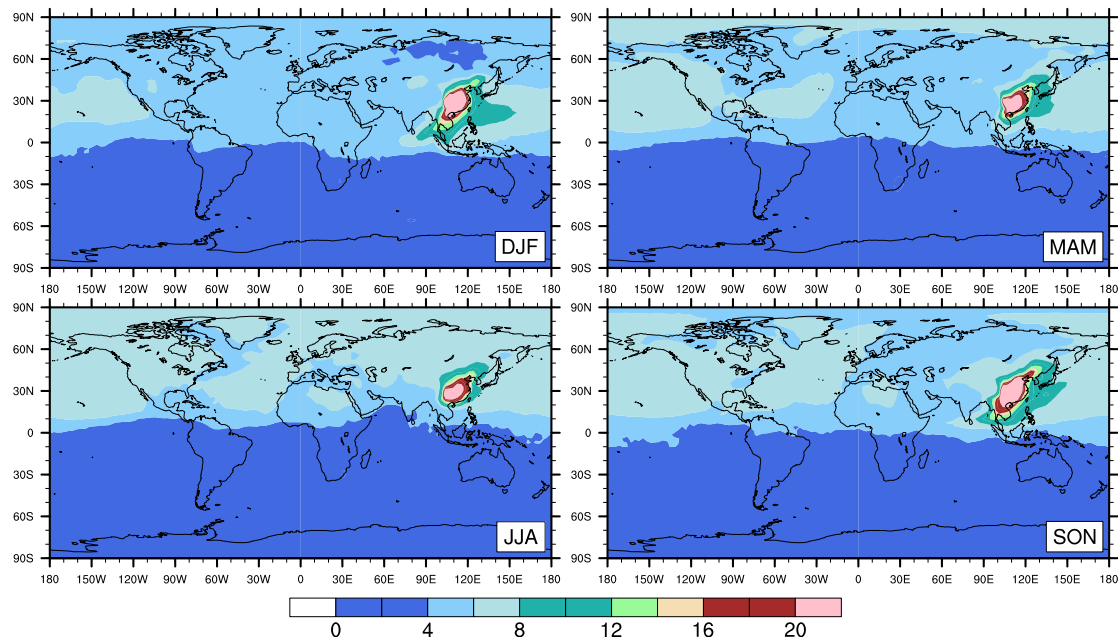
Fig. 12. Percent differences in HGO dry deposition in winter (upper left), spring (upper right), summer (lower left), and fall (lower right) for the *Streets* and *No China* simulations.

Full Screen / Esc

Printer-friendly Version

Interactive Discussion
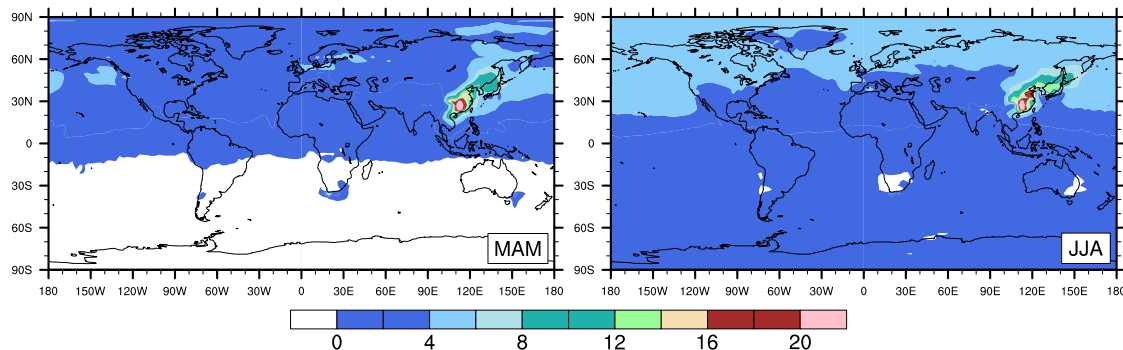
Fig. 13. Percent differences in HGO dry deposition in spring (left) and summer (right) for the *Pacyna* and *Streets* simulations.